A Distributed Control Framework for Integrated Photovoltaic-Battery-Based Islanded Microgrids

Golsorkhi, Mohammad; Shafiee, Qobad; Lu, Dylan Dah-Chuan; Guerrero, Josep M.

Published in:
I E E E Transactions on Smart Grid

DOI (link to publication from Publisher):
10.1109/TSG.2016.2593030

Publication date:
2017

Document Version
Accepted author manuscript, peer reviewed version

A Distributed Control Framework for Integrated Photovoltaic-Battery Based Islanded Microgrids

Mohammad S. Golsorkhi, *Graduate Student Member, IEEE,* Qobad Shafiee*, Member, IEEE*, D.D.C. Lu, *Senior Member, IEEE, and* Josep M. Guerrero*, Fellow, IEEE*

Abstract—This paper proposes a new cooperative control framework for coordination of energy storage units (ESUs), photovoltaic (PV) panels and controllable load units in single-phase low voltage microgrids (MGs). The control objectives are defined and acted upon using a two level structure; primary and secondary control. Unlike conventional methods, a V-I droop mechanism is utilized in the primary control level. A distributed strategy is introduced for the secondary control level to regulate the MG voltage and manage state of charge (SoC) and power among the ESUs. The distributed secondary controllers are coordinated based on a leader-follower framework, where the leader restores the MG voltage to the rated value and the followers manage the sharing of power between the ESUs so as to balance the SoCs. Once the ESUs reach the minimum charge level, the information state increases above a positive critical value, at which point load control units perform load shedding. Similarly, fair PV curtailment is conducted in case the ESUs reach the maximum charge level. Experimental results are presented to demonstrate the efficacy of the proposed method.

***Index Terms*—Distributed control, dispersed storage and generation, inverters, microgrid, secondary control.**

NOMENCLATURE

a_{ij}	Weight of the communication link from unit *j* to *i*
C_i	Capacity of the energy storage unit *i*
E^{rated}	Rated voltage, V
F	SoC function
$F_{\min}$	Lower limit of function *F*
i_o	Output current
k_{lim}	Power limiter coefficient of the leader agent
k_{si}	Distributed secondary controller gain of unit *i*
L_G	Laplacian matrix of the graph G
N_i	Number of the neighbors of agent *i*
P_{oi}	Output active power of DER unit *i*
P_{oi}^{rated}	Rated active power of DER unit *i*
P_{ESUi}	Power generated by energy storage unit *i*
P_{ESUi}^{rated}	Rated power of energy storage unit *i*
P_{PVi}	Power generated by PV unit *i*
P_{marg}	Power margin of the leader agent
$P_{\max i}$	Maximum output power of DER unit *i*
$P_{\min i}$	Minimum output power of DER unit *i*
R_c	Resistance of the DER output inductor
r_d	*d*-axis droop coefficients
r_q	*q*-axis droop coefficients
SoC_i	State of charge of energy storage unit *i*
SoC_L	Lower limit of state of charge
SoC_H	Higher limit of state of charge
$SoC_{\min}$	Minimum permissible state of charge
$SoC_{\max}$	Maximum permissible state of charge
T_{dcom}	Communication delay
v_c^*	DER output voltage reference
v_{si}	Voltage correction term of agent *i*
v_t	DER terminal voltage
w_{ij}	Averaging coefficient
X_c	Reactance of DER output inductor
x_i	Information state of agent *i*
$x_{\max}$	Maximum information state

M.S. Golsorkhi is with the School of Electrical and Information Engineering, University of Sydney, Camperdown NSW-2006, Australia (e-mail: MGOL15@yahoo.com).

Dylan D. C. Lu the School of Electrical, Mechanical and Mechatronic Engineering, University of Technology Sydney, Broadway NSW-2007, Australia (e-mail: Dylan.Lu@uts.edu.au)

Q. Shafiee is with the Department of Electrical and Computer Engineering, University of Kurdistan, Sanandaj, Iran (e-mail: q.shafiee@uok.ac.ir).

J. M. Guerrero is with the Institute of Energy Technology, Aalborg University, Aalborg East DK-9220, Denmark (e-mail: joz@et.aau.dk).

I. INTRODUCTION

The increased penetration of rooftop photovoltaic (PV) panels in low voltage distribution networks might cause several technical problems due to the mismatch between generation and demand throughout the day. Therefore, distribution system operators tend to encourage the installation of energy storage units (ESU) as well as controllable loads, which enable active participation of consumers in load/generation balance [1]. This new infrastructure avails providing the local consumers with a high quality and reliable power source in the context of smart microgrids (MG) [2].

MGs can operate either in the grid connected or islanded modes. During the grid connected mode, voltage and frequency regulation and load/generation balancing are achieved by the upstream network [3]. Therefore, the control schemes are mainly focused on the economical operation, based on energy prices and electricity markets [4]-[6]. During

the islanded mode, however, a more complex control scheme is necessary to ensure stable and reliable operation. In this mode of operation, specifically, the controller is required to 1) maintain load/generation balance, 2) regulate voltage and frequency, 3) balance the state of charge (SoC) of ESUs, 4) protect the inverters and ESUs from power overload, and 5) protect the ESUs from deep discharging or overcharging.

The most straightforward solution for achieving the aforementioned control objectives is using a central power management system [7]-[10]. However, the centralized approach exposes a single point of failure, i.e., any failure in the central controller affects the entire system. Moreover, the implementation of centralized controller requires an extensive and costly communication network [11].

An alternative approach is the decentralized scheme, in which each generation and load unit is controlled by a local controller (LC) [12]-[19]. The conventional decentralized control method uses active power-frequency droop to distribute active power between the distributed energy resources (DERs) [12]. However, the conventional droop method ignores the aforementioned objectives 3-5. Adaptive droop schemes, which change the droop coefficient based on the SoC are proposed to balance the SoCs [13]-[15]. Furthermore, bus signaling strategies are introduced to trigger different mode changing actions thus protecting the ESUs from deep charging and overcharging [16]-[19].

The decentralized solutions are mostly limited to ESU and PV units, which are connected to the grid through separate inverters. To reduce the converter losses and the component costs, a hybrid unit can be formed by connecting the PV and ESU in the DC side of an inverter. Although coordination of a single hybrid unit with other DERs in islanded MGs have been recently studied in [18], [19], the proposed methods are not applicable to MGs consisting of multiple hybrid units. In addition, the decentralized methods suffer from frequency and voltage deviations, which degrade the power quality.

Distributed control is a solution to address the limitation of centralized and decentralized approaches in implementation of the energy management system. The distributed control frameworks are comprised of local control agents, which are interconnected through a sparse communication network [20]. These control strategies are mostly based on consensus protocols, which enable regulating some local parameters e.g., voltage, frequency or power generation to a global average value [21]. The distributed control methods favor improved reliability, expandability and lower communication cost compared to the centralized control methods [22].

Distributed control methods have recently gained attraction in various area of microgrid control, e.g., for the elimination of voltage and frequency deviations caused by the primary droop controllers [21]-[25], load power sharing [25], economic profitability [26], voltage control [27], [28], and SoC balancing [29]-[31] as main ones. However, there is not a single work in the literature, using the potential of distributed control mechanism for coordination of hybrid PV-ESU units in islanded MGs. In this paper, a novel distributed control framework is proposed to manage the state of each generation/load unit according to the aforementioned control objectives. The main contributions of this paper are as follows:

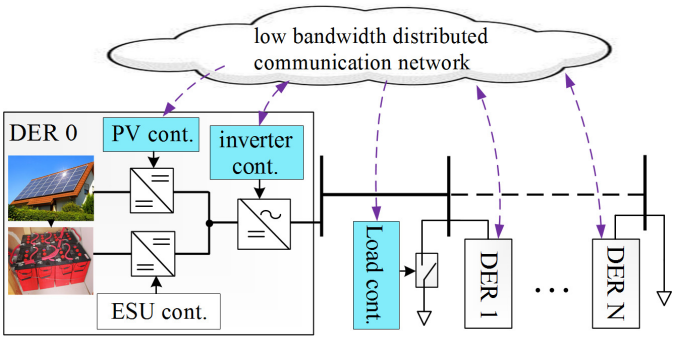

Fig. 1. General schematic of the MG control architecture.

1. In contrast with the existing methods in [12], [13], where coordination of a single hybrid PV-ESU unit with the other DERs is studied, our proposed approach enables coordinated control of MGs consisting of multiple hybrid PV-ESU units.
2. A new consensus-based leader-follower strategy is introduced which dynamically changes the communication network topology to ensure SoC balancing despite the power constraints. The leader regulates the voltage in the whole MG, while the followers are responsible to manage the power sharing among the ESUs in the MG. In contrast with the control method in [23], which incorporates the SoC management objective in active power-frequency droop characteristics and use the distributed controller mitigate the frequency drifts, we use our current sharing method (proposed in [32]) for power distribution and directly incorporate the SoC management into the distributed control algorithm. The works in [27] and [28] propose similar leader-follower methodology, but for overvoltage protection during grid-connected mode of operation and are not applicable to the islanded MGs. As opposed to the proposed method, the control schemes in [29]-[31] do not consider SoC and power constraints.
3. A distributed load shedding and PV curtailment strategy is adapted to assure the SoCs are maintained within safe operating region.

The rest of the paper is organized as follows. The control layout is presented in Section II. The proposed control method is detailed in Sections III and IV. Experimental results are presented in Section V to verify the efficacy of the method. Section VI concludes the paper.

II. Controller Layout

Consider the MG of Fig. 1, which is composed of single-phase hybrid DERs and controllable and uncontrollable loads connected to a LV feeder. Each DER is supplied by a rooftop PV panel and an ESU, which are connected to a common DC bus through DC/DC boost converters. The DER is interfaced with the MG through a single phase inverter.

Each of the converters and controllable loads are controlled by a separate module. The ESU control module regulates the DC bus voltage. The PV control module normally adjusts the PV current based on maximum power point tracking method.

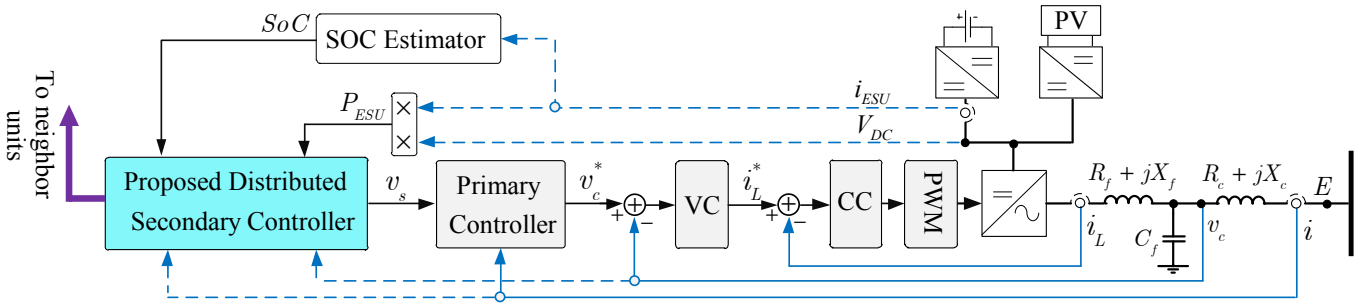

Fig. 2. Schematic of the inverter control module

If the ESUs in the MG are charged to the maximum level, the PV controllers are switched to power curtailment mode to reduce the PV generation. The inverter control module manages the output power based on the total load, total PV generation and SoC of all units. The load control module performs load shedding in case the ESUs are discharged to the minimum level.

The control modules, which are also referred to as control agents, are interconnected through a low bandwidth distributed communication network. The control framework must ensure load/generation balance, maximize the PV generations, balance the SoCs and regulate the voltage. In addition, the following constraints need to be satisfied:

$$SoC_{\min} < SoC_i < SoC_{\max} \tag{1}$$

$$\left|P_{oi}\right| < P_i^{rated} \tag{2}$$

$$\left|P_{ESUi}\right| < P_{ESUi}^{rated} \tag{3}$$

The controller should be independent from the network topology and robust with respect to parameter/load variations and communication interrupts. The control structure is detailed in the following Sections.

III. Inverter Control Module – Primary Level

As shown in Fig. 2, the inverter control module is based on a cascaded structure. The inner loop voltage (VC) and current controllers (CC) use proportional plus resonant method to track the reference voltage with a fast dynamic response. The primary controller adopts V-I droop characteristic to enable decentralized coordination of the DERs.

The V-I droop method uses GPS timing technology as a time stamp for synchronizing the DERs to a global synchronous reference frame [33]. Therefore, the MG frequency is fixed at the nominal value. In this framework, the *d* and *q* components of the DERs currents are coordinated by using the following V-I droop control law [34]

$$\begin{bmatrix} v_{cd}^* \\ v_{cq}^* \end{bmatrix} = \begin{bmatrix} E^{rated} \\ 0 \end{bmatrix} + \begin{bmatrix} R_c & -X_c \\ X_c & R_c \end{bmatrix} \begin{bmatrix} i_{od} \\ i_{oq} \end{bmatrix} - \begin{bmatrix} r_d & 0 \\ 0 & r_q \end{bmatrix} \begin{bmatrix} i_{od} \\ i_{oq} \end{bmatrix} \tag{4}$$

The second term on the right hand side of (4) is introduced to compensate the voltage drop across the output inductor. The third term is the droop voltage, which acts like a virtual resistance [35]. It should be noted that direct control of current (instead of power) improves the dynamic response [36]. Moreover, the introduction of a resistance-based droop makes the method suitable for low voltage MGs where networks have resistive impedance in practice.

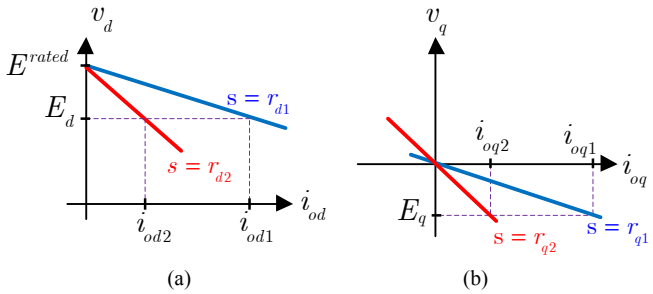

Fig. 3. V-I droop mechanism: a) d axis and b) q axis

Although the V-I droop scheme is based upon the use of GPS receivers for time synchronization, such requirement can be removed by replacing the GPS with a Q-f droop characteristic as shown in [37]. Therefore, it is also possible to implement the proposed scheme without GPS receivers.

The operation of V-I droop mechanism for a MG composed of two DERs with different power rating is demonstrated in Fig. 3. At no-load conditions, the DERs currents are zero and the PCC voltage is regulated at E^{rated}. When the load is increased, the voltage drops and the load power is shared between the DERs according to the droop coefficients, i.e., r_{di} and r_{qi}. It is observed that the DER with smaller droop coefficient delivers higher current. Thus, it is possible to evenly share i_{od} and i_{oq} between the DERs by properly selecting the droop coefficients. Since $E_d \approx 1pu$ and $E_q \approx 0$, the active and reactive powers are proportional to i_{od} and i_{oq}, respectively. As a result, the active and reactive powers are also shared evenly between the DERs. The interested readers are referred to [32] for more details about V-I droop mechanism.

IV. Inverter Control Module – Secondary Level

In this section, a novel distributed secondary control (DSC) method based on the consensus concept is proposed to achieve the objectives of SoC balancing, restoring the voltage to the nominal value and ensuring safe operation.

A. Fundamentals of Consensus control strategy

Consensus concept [38] is used to implement the DSC. In this context, each unit is regarded as a control agent which is connected to its direct neighbor through a sparse

communication network. The communication network may form a weighted graph, where the agents and communication links are represented by nodes and edges, respectively. The interaction between the agents in this cyber network is quantified in terms of the graph adjacency matrix, $A_G = [a_{ij}] \in R^{(N+1)*(N+1)}$, in which $N+1$ is the total number of agents. In case the agent i receives information from agent j, $a_{ij} > 0$ and otherwise, $a_{ij} = 0$. A scalar information state, x_i, is assigned to each agent.

A well-established method for coordination of the agents is to update the state of agent i according to

$$\dot{x}_i = \sum_{j=0}^{N} a_{ij} \left(x_j - x_i \right) \tag{5}$$

Equation (5) is commonly referred to as a distributed consensus algorithm in the literature, since it guarantees convergence to a collective decision via local interactions [39]. Defining the convex coefficients $w_{ij} = a_{ij} / \sum_{k=0}^{N} a_{ik}$, one can rearrange (5) as

$$\frac{1}{\sum_{k=0}^{N} a_{ik}} \dot{x}_i = -x_i + \sum_{j=0}^{N} w_{ij} x_j \tag{6}$$

Therefore, the information state of agent i converges to a weighted average of the information states of its neighbors [40]. If the distributed communication network contains minimum connectivity, each of the information states will converge to a common value: $x_0 = x_1 = \ldots = x_N$ [38].

Although each of the agents can serve as a virtual leader, it is preferable to select the agent which has the least electrical distance from the critical bus of the MG as the leader [39]. Without loss of generality, agent 0 is assigned as the leader and other agents are assigned as followers. The leader does not receive information from the follower agents; thus $a_{0j} = 0$. The follower agent i receives information from its immediate neighbors and the leader (i.e. agent 0).

B. SoC Balancing

The proposed distributed secondary controller (DSC) realizes the consensus method by introducing a voltage correction term, v_s, into the d-axis droop characteristics. The mechanism of operation of the DSC is explained based on the simplified model of Fig. 4. In this model, the dynamics of the VCs, CCs and LCL filters are neglected due to their small time constant compared to the secondary controller. Consequently, the V-I droop controller is simplified to the combination of a voltage source (E^{rated}) and a virtual resistance (r_d). The DSC voltage correction term is represented as a dependent voltage source.

In case the DSC voltage correction terms are zero, the load power is shared between the DERs according to the V-I droop virtual resistances. Additionally, the MG voltage profile deviates from the rated value due to the drop on the virtual resistances as well as the distribution lines. The voltage profile can be improved by setting the DSC offsets of all units to an appropriate common value. However, such a strategy

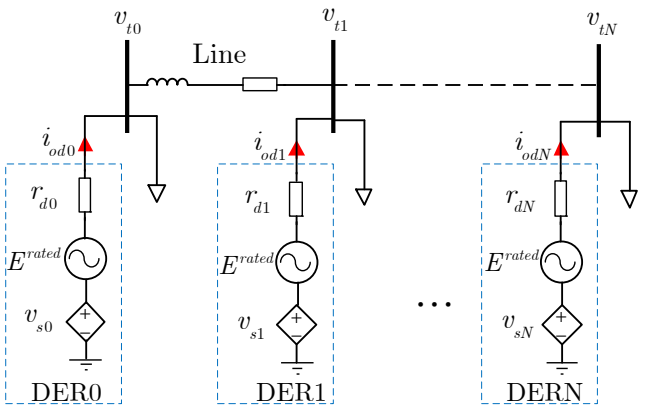

Fig. 4. Simplified MG model.

keeps the power sharing between the units unaffected. In order to improve the voltage profile while achieving SoC-dependent power sharing, the DSC voltage correction terms are controlled according to a leader-follower strategy, as explained in the following.

To improve the voltage profile, the leader voltage correction term is calculated as

$$v_{s0} = k_{s0} \int \left(E^{rated} - v_{t0} \right) dt \tag{7}$$

With the intention of SoC balancing, the information state of unit i is defined as

$$x_i = \overbrace{\frac{P_{ESUi}}{C_i}}^{\text{normalized ESU power}} \times \overbrace{\frac{1}{F\left(SoC_i\right)}}^{\text{SoC-dependent coefficient}} \tag{8}$$

The function $F()$ is defined as

$$F\left(SoC_i\right) = \begin{cases} SoC_i - SoC_L & \text{if } P_{ESUi} \geq 0 \\ SoC_H - SoC_i & \text{if } P_{ESUi} < 0 \end{cases} \tag{9}$$

For the follower unit i, the voltage correction term, v_{si}, is

$$v_{si} = k_{si} \int \left(P^*_{ESUi} - P_{ESUi} \right) dt \tag{10}$$

in which the ESU reference power, P^*_{ESUi}, is calculated according to a weighted average of the neighbors' information states, i.e.,

$$P^*_{ESUi} = C_i F\left(SoC_i\right) \sum_{j=0}^{N} w_{ij} x_j \tag{11}$$

in which the coefficients w_{ij} are defined as

$$w_{ij} = \begin{cases} \dfrac{1}{N_i} & \text{if agent } i \text{ receives data from agent } j \\ 0 & \text{otherwise} \end{cases} \tag{12}$$

Comparison of equations (7) and (10) reveals that the leader attempts to restore the voltage to the nominal value while the followers pursue altering the load sharing between the DERs.

Combining (8), (10) and (11), the voltage correction term of

the follower agent *i* is expressed as

$$\dot{v}_{si} = k_{si} C_i F\left(SoC_i\right)\left(-x_i + \sum_{j=0}^{N} w_{ij} x_j\right) \tag{13}$$

Simplifying (13), one can notice that the proposed distributed secondary algorithm is in fact a special form of the well-known consensus protocol in (6).

From the model of Fig. 4, one can write the DER output current

$$i_{odi} = \frac{E^{rated} + v_{si} - v_{ti,d}}{r_{di}} \tag{14}$$

In addition, neglecting the converter losses, the output current is related to the ESU power, i.e.,

$$i_{odi} \cong \frac{P_{ESUi} + P_{PVi}}{v_{ti,d}} \tag{15}$$

Combining (14) and (15), the relation between the voltage correction term and ESU power is obtained

$$v_{si} \cong \frac{r_{di}}{v_{ti,d}} P_{ESUi} + \left(r_{di}\frac{P_{PVi}}{v_{ti,d}} + v_{ti,d} - E^{rated}\right) \tag{16}$$

Replacing P_{ESUi} with $x_i C_i F(SoC_i)$ (as per (8)), (16) can be expressed as

$$v_{si} \cong \frac{r_{di} C_i F\left(SoC_i\right)}{v_{ti,d}} x_i + \text{constant} \tag{17}$$

where the PV power and the grid voltage are assumed constant. Substituting (17) in (13), the dynamics of the DSC are represented as

$$\frac{r_{di}}{k_{si} v_{ti,d}} \dot{x}_i = -x_i + \sum_{j=0}^{N} w_{ij} x_j \tag{18}$$

Equation (18) is a special form of (6) with coefficients a_{ij} selected as

$$a_{ij} = \begin{cases} \dfrac{1}{N_i}\dfrac{k_{si} v_{ti,d}}{r_{di}} & \text{if agent } i \text{ receives data from agent } j \\ 0 & \text{otherwise} \end{cases} \tag{19}$$

As mentioned in Section III-A, when the consensus strategy converges, all of the information states will reach to a common value. Therefore, (8) and (9) imply that the surplus power (i.e., total PV generation minus total load) during discharging and charging modes will be dispatched between the DERs according to

$$\frac{P_{ESU0} / C_0}{SoC_0 - SoC_L} = \cdots = \frac{P_{ESUN} / C_N}{SoC_N - SoC_L} \tag{20}$$

$$\frac{P_{ESU0} / C_0}{SoC_H - SoC_0} = \cdots = \frac{P_{ESUN} / C_N}{SoC_H - SoC_N} \tag{21}$$

Consequently, the ESU with higher SoC is discharged faster (charged slower) than the one with lower SoC [29].

C. Controller design guidelines

The criteria for the controller design are:

1. The dynamics of the DSC should be much slower compared to the primary control level but much faster compared to the rate of change of SoCs.
2. The proposed consensus algorithm must be stable in spite of the communication constraints.

The first criterion ensures the decoupling of primary and secondary control levels. As detailed in [32], the time constant of the V-I droop controller is around one fundamental cycle, i.e., 20ms. On the other hand, the rate of change of SoC is in the order of minutes-hours. Therefore, the time constant of the DSC should be in the order of seconds.

The effect of communication constraints including the delays and the switching of topology on the consensus algorithm is detailed in [41] and [42]. Defining the Laplacian matrix of the communication network, $L_G = [l_{ij}] \in R^{(N+1)*(N+1)}$, as

$$l_{ij} = \begin{cases} \sum_{k=0,k\neq i}^{N} a_{ik} & \text{if} \quad i = j \\ -a_{ij} & \text{otherwise} \end{cases} \tag{22}$$

the consensus algorithm will converge if the communication delay satisfies the following inequality [41]:

$$T_{dcom} < \frac{\pi}{2\lambda_{\max}\left(L_G\right)} \tag{23}$$

in which $\lambda_{\max}$ refers to the largest eigenvalue of a matrix.

To simplify the design, all nonzero communication coefficients are selected to be identical and equal to *a*. Using the theorem proposed in [43], an upper bound for the largest eigenvalue of Laplacian matrix is expressed as

$$\lambda_{\max}\left(L_G\right) \le \left(2\max_i\{N_i\} - 1\right)a \tag{24}$$

Substituting (24) into (22), the upper bound of the communication coefficient is calculated as

$$a < \frac{\pi}{\left(4\max_i\{N_i\} - 2\right)T_{dcom}} \tag{25}$$

Combining (25) and (19), the upper bound of the DSC gain for agent *i* is obtained as

$$k_{si} < \frac{r_{di}}{v_{ti,d}} \frac{\pi N_i}{\left(4\max_i\{N_i\} - 2\right)T_{dcom}} \tag{26}$$

D. Power Limiting

Although the proposed distributed method in Section IV-B is effective in terms of SoC balancing, it does not respect the power limits of inverters and ESUs. In order to guarantee safe operation, the proposed consensus algorithm is modified to

comprise the power limiting feature.

The minimum and maximum limits of the ESU power are obtained by combining (2) and (3)

$$P_{\min i} = max\left\{-P_{oi}^{rated} - P_{PVi}, -P_{ESUi}^{rated}\right\} \quad (27)$$

$$P_{\max i} = \min\left\{P_{oi}^{rated} - P_{PVi}, P_{ESUi}^{rated}\right\} \quad (28)$$

For the follower agents, the ESU reference power, which is calculated from (11), is checked versus the maximum and minimum limits, i.e.,

$$P_{\min i} \le P_{ESUi}^{*} \le P_{\max i} \quad (29)$$

If the constraint (29) is violated, the ESU power is fixed at the corresponding limit. This means that the variable x_i is also fixed. In such a case, the agent i is excluded from the algorithm and does not broadcast its state information to the other agents. In order to ensure the integrity of the communication network, the agent is bypassed by sending the information state of agent i-1 to the agent i+1 and vice-versa.

For the leader agent, ESU power limiting is conducted by amending the information state, as follows

$$x_0 = \begin{cases} \dfrac{P_{ESU0}}{C_0 F(SoC_0)} + k_{lim}\left(P_{ESU0} - P_L\right) & \text{if } P_{ESU0} < P_L \\ \dfrac{P_{ESU0}}{C_0 F(SoC_0)} & \text{if } P_L < P_{ESU0} < P_H \\ \dfrac{P_{ESU0}}{C_0 F(SoC_0)} + k_{lim}\left(P_{ESU0} - P_H\right) & \text{if } P_{ESU0} > P_H \end{cases} \quad (30)$$

in which $P_L = P_{min0} + P_{marg}$, $P_H = P_{max0} - P_{marg}$.

The power margin, P_{marg}, is a key design parameter; large power margin reduces the functionality of the proposed SoC balancing method, while small values adversely affect the controller dynamics. The parameter k_{lim} is designed based on the following criteria

$$k_{\lim} > \frac{P_{marg}}{x_{\max}} \quad (31)$$

Combining (30) and (31), it can be inferred that as long as $x_0 < x_{\max}$, the ESU power remains within the limits.

If the ESU power is within the defined margins, (30) is reduced to (8) and the leader power is determined based on its SoC. Otherwise, the magnitude of the leader information state is increased, imposing other agents to increase their share of surplus power. As a result, the leader power is limited.

E. Proposed DSC algorithm

Fig. 5 illustrates the cooperative algorithm for the leader agent. As can be seen, the terminal voltage of the inverter is estimated first according to the simplified DER model (see Fig. 4). To restore the voltage drop caused by the primary droop controller, the leader control command is updated based on (7). Next, the function $F(SoC_0)$ is calculated according to (9) and limited to the range $[F_{\min}, \infty)$. This restriction is necessary to prevent the information state from singularity.

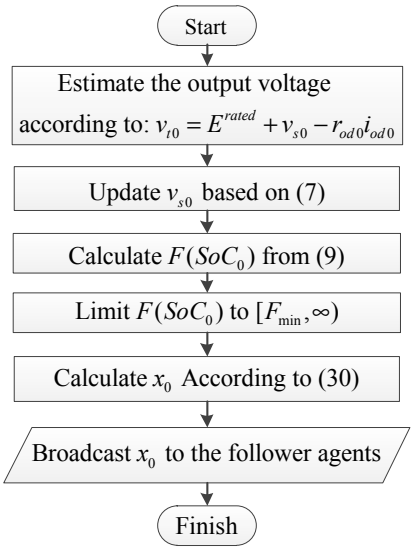

Fig. 5. Flowchart of the proposed cooperative algorithm for the leader agent.

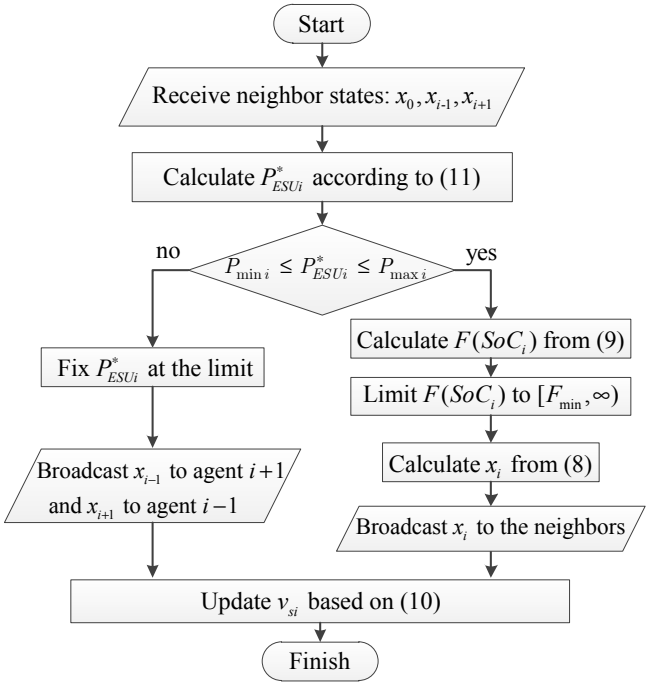

Fig. 6. Flowchart of the proposed cooperative algorithm for follwer agents.

Following, the information state is obtained according to (30) and broadcasted to the follower agents.

The consensus algorithm for the follower agent i is shown in Fig. 6. The agent i receives information from its immediate neighbors (agent i-1 and agent i+1) and the leader. The ESU reference power required for SoC balancing is calculated using (11). The algorithm then checks whether the reference power is in the safe operating range. If the reference power is within the safe range, $F(SoC_i)$ is calculated, and limited to $[F_{\min}, \infty)$. The information state x_i, is estimated according to (8) and broadcasted to the neighbor agents. Once the ESU reference power, P_{ESUi}^{*}, is out of the safe operating range, the power set point is fixed at the limit and the agent is bypassed by sending the information state of agent i-1 to the agent i+1 and vice-versa. Finally, the secondary voltage correction term is updated based on (10).

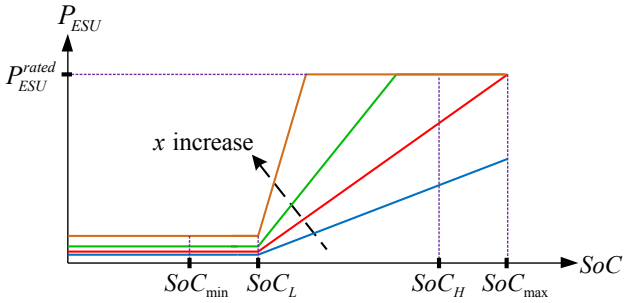

Fig. 7. Variations of ESU current versus SoC for different values of x.

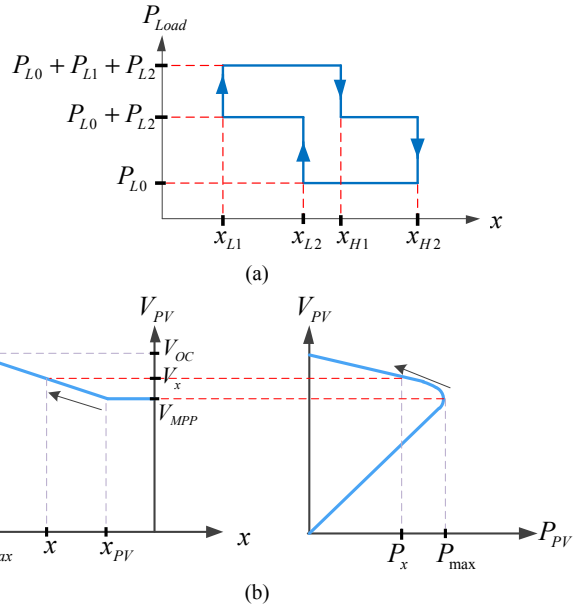

Fig. 8. Control characteritics of a) load control and b) PV control modules.

V. Load and PV Control Modules

The loading and PV generation capacity of the MG is limited not only by the power rating of the DERs but also the SoC constraints. During night time (i.e., no PV generation), the total loading capacity is the summation of the rated power of the ESUs which are charged above the minimum SoC. During day time, the total PV generation capacity is the summation of rated power of ESUs which have not reached the maximum SoC minus the total load. In order to maintain load/generation balance while preventing ESUs from deep discharging and overcharging, a load shedding and PV curtailment method is introduced in this Section.

The loads and PVs are controlled based on the average information state of the leader, which is approximately equal to the steady-state information state of all DERs, i.e., x. The operating principle of the load control module is explained based on the diagram shown in Fig. 7. The diagram illustrates the variation of ESU current versus SoC for different values of x as a parameter. It is worth mentioning that the margin between SoC_L (SoC_H) and the minimum (maximum) SoC provides a reserve capacity for supplying sensitive loads and managing the transients. For small value of x, the current is shared between the ESUs according to the SoCs, while the current of ESUs with $SoC < SoC_L$ is negligible. However, as x rises, the DERs with higher SoC reach their current limit. As

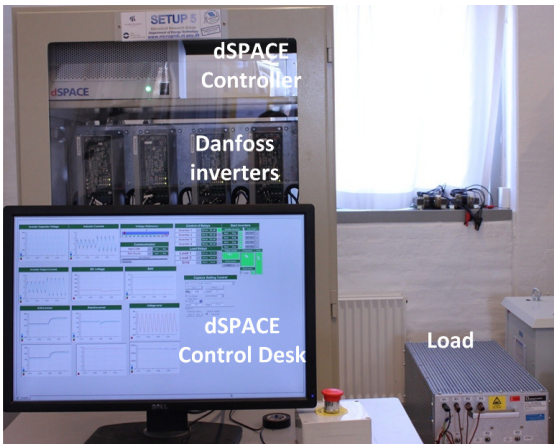

(a)

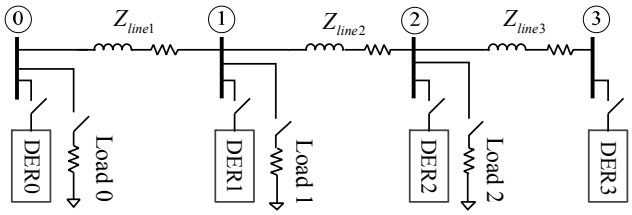

(b)

Fig. 9. Experimental setup: a) hardware and b) schematic diagram.

a result, ESUs with lower SoC discharge faster than expected, quickly reaching the minimum charge level. Therefore, it is necessary to shed some part of the MG load in case that x is higher than a positive critical level. Once x is lower than a negative critical level, PV generations must be curtailed.

The load shedding is conducted based on a hysteresis characteristic to prevent chattering phenomenon. As an example, the load shedding characteristics for a MG consisting of two controllable loads is shown in Fig. 8(a). When x rises above the level x_{H1} or x_{H2}, local loads 1 or 2 are disconnected, respectively. The loads 1 and 2 remain disconnected until x falls below x_{L1} and x_{L2}. Therefore, the chattering phenomenon is prevented.

The PV curtailment characteristic is shown in Fig. 8(b). Normally, the PV generations are controlled by maximum power point (MPP) tracking method. As can be observed, once x is decreased below x_{PV}, the PV voltage is increased to reduce the PV generation. Using an identical characteristic for all PV control modules, fair curtailement can be ensured.

VI. Experimental Results

The proposed method has been tested on a laboratory scale MG setup depicted in Fig. 9. The test bench was prototyped in the Intelligent Microgrid Laboratory at Aalborg University [44]. The specifications of the experimental setup are listed in Table I. The underlying MG setup includes four single-phase DER units. Each DER unit is composed of a Danfoss 700 W inverter and an LCL filter which is installed to reduce the switching-induced harmonics. The inverters are supplied by a programmable DC source. The DERs and loads are interconnected through a resistive distribution network model (see Table I). A dSPACE 1006 digital control system is used to implement the controller routines as well as modelling the GPS synchronization and communication network. The ESUs,

TABLE I. ELECTRICAL AND CONTROL PARAMETERS OF THE TEST MG

	Parameter	Symbol	Value
Test Specifications	Nominal phase voltage	E^{rated}	220 Vrms
	Nominal Frequency	f^{rated}	50 Hz
	Filter parameters	L_f/ C_f/ L_c	3.6mH/ 9μF /3.6mH
	Line 1 impedance	Z_{line1}	0.18 +j0.07 Ω
	Line 2 impedance	Z_{line2}	0.28+j0.08 Ω
	Line 3 impedance	Z_{line3}	0.38+j0.06 Ω
	Load impedance: case 1-3	R_0/ R_1/ R_2	115 /57 /57 Ω
	Load impedance: case 4	R_0/ R_1	230 / 115 Ω
	Load impedance: case 5	R_0/ R_1/ R_2	115 /115 /57 Ω
	SoC constraints	SoC_{min} -SoC_{max}	50-100 %
	ESU capacities	C_0 /C_1 /C_2 /C_3	2.8/4.2/5.6/2.5 kW-min
	Communication Rate	f_{com}	50 samples/s
	Communication delay	T_{dcom}	20 ms
Control Parameters	Leader DSC	k_{s0}	1
		k_{lim}	0.1
		P_{marg}	200 W
	Follower DSC	k_{si}	0.014
	Function F	F_{min}	0.01
	SoC limits	SoC_L-SoC_H	55-95%
	PV control thresholds	x_{PV}/ x_{max}	-10/15
	Load 1 control thresholds	x_{L1} - x_{H1}	0.1 -10
	Load 2 control thresholds	x_{L2} - x_{H2}	1 - 15
	Droop coefficients	r_d/ r_q	4 / 8.4 Ω

PVs and the corresponding DC/DC converter are modeled in MATLAB and emulated in the dSPACE controller.

Efficacy of the proposed control method is verified under the following studies: 1) DSC performance assessment, 2) step load reponse, 3) discharge cycle scenario, 4) day time scenario, and 5) impact of communication delay.

In the first, second and third study, the PV generations are zero and the load is supplied by the ESUs. The experimental results for the first study are provided in Fig. 10. Prior to activating the proposed controller, the load active power is shared among the units by means of the V-I droop mechanism. At *t=5s*, the DSC is activated, where the power set point of each inverter is adjusted so as the information states of the units reach a common value. As shown in Fig. 10 (c), the consensus is reached within 10s after activation of the DSC. As a consequence, the set points of inverters' powers are defined according to the SoC and capacity of the ESUs. Particularly, the largest share is dedicated to DER2; the one which has the highest stored energy (SoC=95% and C= 5.6 kW.min), followed by DER1 (SoC=99% and C=4.2 kW.min).

Comparison of Fig. 10 (b) and 10(c) reveals that the DSC transient response is much faster compared to the rate of change of SoCs. Therefore, the proposed method is effective in terms of SoC balancing. Additionally, the output voltage of the leader i.e., DER0 is restored to 1pu (See Fig. 10 (d)).

In the second test, the response of the system to a step load change is studied by connecting the load 1 to the MG. From Fig. 11(a), it is observed that the active powers of all units rise following the step load change. Since the SoC of DER0 is lower compared to other units, its information state (*x*0) grows rapidly (See Fig. 11(b) and 11(c)). Consequently, *P1* and *P2* are increased to reduce *P0* and consensus is achieved within 10s. As shown in Fig. 11(d), the DERs output voltage are regulated within a range of the nominal value. The slight

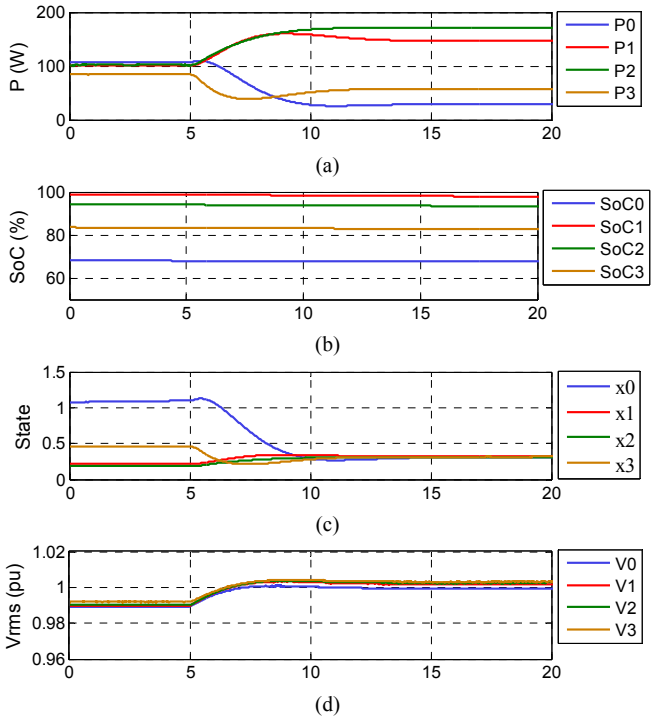

Fig. 10. Perfromance of the proposed method following the DSC activation. (a) inverters' active powers, (b) SoCs, (c) information states, (d) bus voltages.

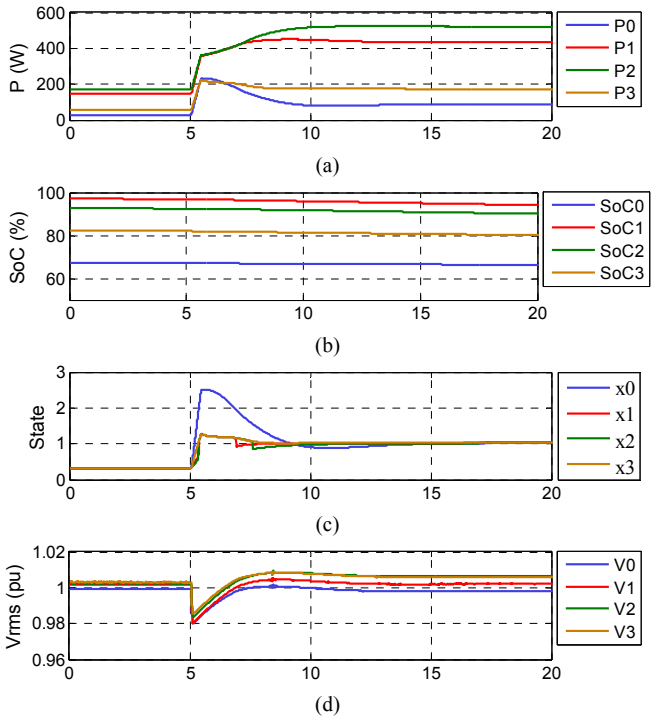

Fig. 11. Controller performance in response to a step load change. (a) inverters' active powers, (b) SoCs, (c) information states, (d) bus voltages.

voltage deviation of the follower units originates from the voltage drop on the line impedances.

The third scenario studies the performance of the proposed control framework over the ESUs discharge cycle. Initially, loads 0 and 1 are connected to the MG. As shown in Fig. 12, the information states are at consensus and the load is shared among the DERs according to the corresponding energy capacities. Once load 2 is connected at $t = 20\,\mathrm{s}$, *P1* and *P2*

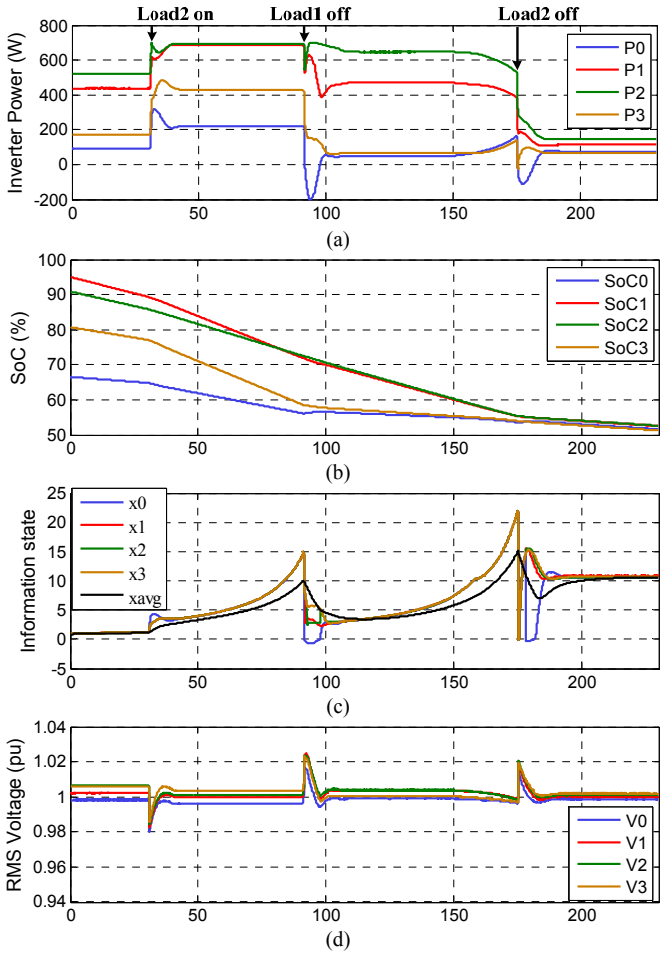

Fig. 12. Experimental results for the third scenario. (a) active powers, (b) SoCs, (c) average information state, and d) bus voltages.

reach their limits, and their powers are fixed at 700 W. This results in an inevitable increase in *P3* and *P0*. Consequently, the SoC3 and SoC0 fall with a relatively fast rate until $t = 80\,\mathrm{s}$, when SoC0 reaches close to the lower SoC limit (i.e., SoC_L=55%). At this point, the average information state, i.e., *xavg*, reaches the trigger point of load 1 (i.e., $x_{H1} = 10$). It is worth mentioning that the delay of *xavg* compared to the agents' states (*x*0-*x*3) is caused by the low-pass filter used for preventing load shedding during transients. The load controller sheds load 1, and subsequently DER 1 and DER 2 exit the power limiting mode, enabling SoC-based load sharing once again. Therefore, the SoCs converge towards SoC_L. At $t = 165\,\mathrm{s}$, all SoCs reach $\mathrm{SoC_L}$ and the information state *xavg* reaches the trigger point of load 2 (i.e., $x_{H2} = 15$). Accordingly, load 2 is also shed from the MG. At this stage, the MG only supplies the sensitive load (i.e., load 0). It should be noted that once all SoCs reach the minimum value (50%) the MG has to be shut down to prevent deep discharging of the ESUs.

In the fourth study, PV generations vary according to a typical profile. Fig. 13 illustrates the experimental results for this study. The effect of PV alignment on the received energy is modeled by considering time shifted irradiations, as depicted in Fig. 13 (b). Prior to $t = 70\,\mathrm{s}$, the total PV generation is lower than the total load, and the excess demand is shared between the ESUs. For $t > 70\,\mathrm{s}$, the total PV

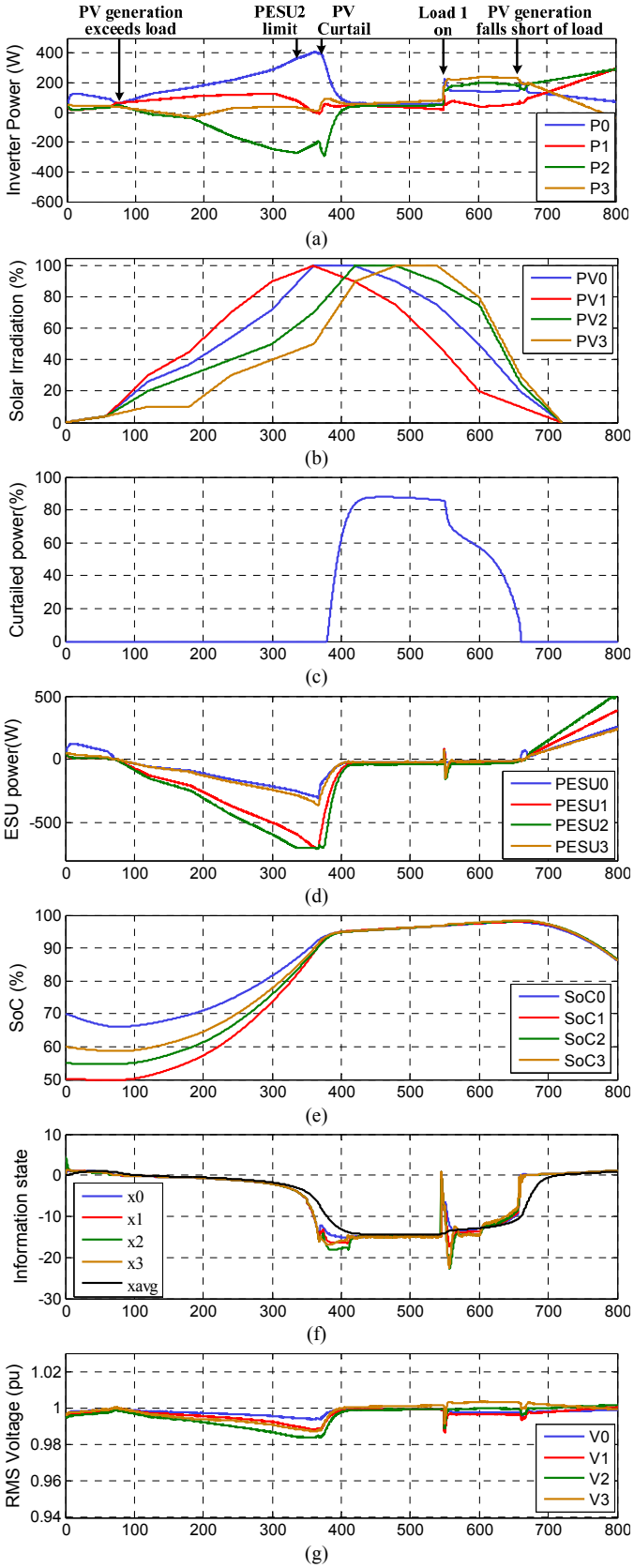

Fig. 13. Perfromance of the proposed control framework for the day scenario. (a) inverters' active powers, (b) solar irradiations, (c) curtailed pv power, (d) ESU powers, (e) SoCs, (f) information state, and (g) bus voltages.

generation goes higher than the total load and the surplus generation is shared among the ESUs according to the available storage capacity. Particularly, the largest share is

dedicated to PESU2 (SoC2=55%, C2=5.6 kW.min) followed by PESU1 (SoC1=50%, C1=4.2 kW.min). For $340\,\mathrm{s} < t < 375\,\mathrm{s}$, PESU2 reaches the limit and remains fixed at -700 W. At $t = 380\mathrm{s}$, the SoCs reach close to the higher SoC limit (95%) and the average information state drops below x_{PV} (i.e., -10). At this stage, the PV control modules increase the voltages to reduce the PV generations so as to keep the surplus generation close to zero. As a result, the ESU powers are decreased to around zero and the SoCs are limited below 100%.

At $t = 550\,\mathrm{s}$, the load 1 is switched on. The load change is initially picked up by the ESUs. However, the increase of ESU powers results in a rise of information states. As shown in Fig. 13 (f), the information states undergo an oscillation but settle at a common value within 20s. The load change causes the average information state (*xavg*) to change from -14.3 to -13.1. Therefore, the PV control modules increase the PV generations to reduce the ESU power back to around zero. The PV control modules continue increasing the PV powers in order to keep the surplus power generation close to zero. At $t = 670\,\mathrm{s}$, the PV generations are increased to the maximum and hence the PVs are controlled at MPPT. Next, the maximum PV generation drops below the total load due to the low solar irradiance. Therefore, the ESUs powers are increased to maintain load/generation balance. It is worth mentioning that in both case studies (see Fig. 12(d), and Fig. 13(g)), the rms voltage is within an acceptable range of the rated value and the frequency is fixed at 50Hz. Therefore, a high power quality is guaranteed.

In the fifth case, effect of communication delay on the performance of the proposed cooperative method is studied. To that end, a step load change is applied to bus 2 and the dynamic response with three different communication delays is recorded. The active power outputs and the information states of the DERs for communication delays of 20 ms, 200 ms and 1 s are depicted in Fig. 14. The results show that for delays shorter than 1 s, the proposed controller remains functional. Although large delays may cause low frequency oscillations, the settling time is fast enough for the SoC management application.

VII. Conclusions

In this paper, a novel distributed control framework is proposed for MGs comprising of several PV-ESU hybrid units. In the proposed method, the individual units are controlled by decentralized V-I droop mechanism together with dedicated distributed secondary controller, which are interconnected through a low bandwidth communication network. The distributed controllers are coordinated based on a leader-follower framework, where the leader regulates the voltage and the followers manage the sharing of power between the ESUs so as to balance the SoCs. The communication topology is dynamically changed to exempt the units which reach the maximum power from the consensus algorithm. In addition, PV curtailment and load shedding are deployed to protect the ESUs from deep discharging and overcharging. Therefore, safe operation of the ESUs and

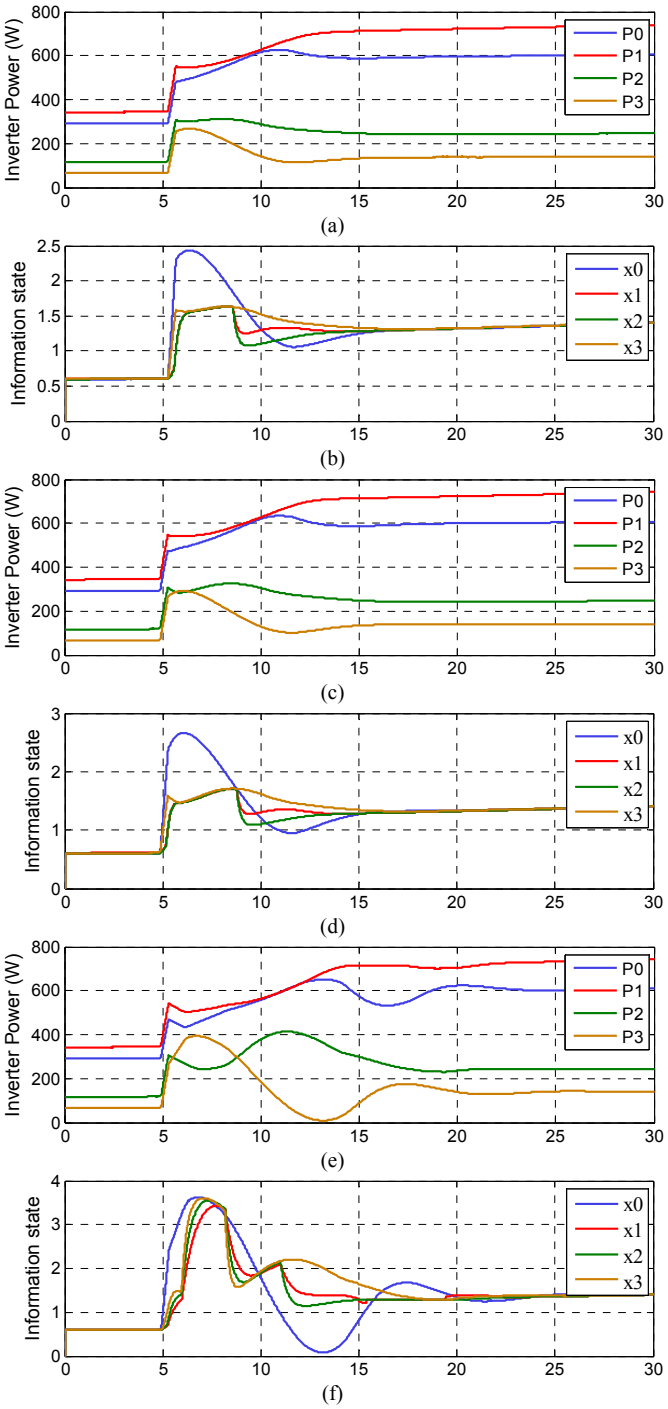

Fig. 14. Performance of proposed control method under different communication delays: (a,b) 20 ms, (c,d) 200 ms, and (e,f) 1 s.

associated DC/DC and DC/AC converters is guaranteed. The experimental results validate the efficacy of the proposed method in terms of voltage regulation, SoC balancing, and limiting the SoCs/ powers within the safe range. The results also show that the proposed control framework is robust with respect to large communication delays.

The proposed method opens up a new way for the integration of SoC and power constraints of hybrid PV-ESU units in the consensus strategy. The next step is coordination of current harmonics considering current limits and THD constraints.

REFERENCES

[1] A. Ipakchi and F. Albuyeh, "Grid of the future," *IEEE Power Energy Mag.,* vol. 7, pp. 52-62, Jan. 2009.

[2] A. Purvins, H. Wilkening, G. Fulli, E. Tzimas, G. Celli, S. Mocci, *et al.*, "A European supergrid for renewable energy: local impacts and far-reaching challenges," *J CLEAN PROD,* vol. 19, pp. 1909-1916, Nov. 2011.

[3] M. Zhixin, X. Ling, V. R. Disfani, and F. Lingling, "An SOC-Based Battery Management System for Microgrids," *IEEE Trans. Smart Grid,* vol. 5, pp. 966-973, Mar. 2014.

[4] A. Hooshmand, B. Asghari, and R. K. Sharma, "Experimental Demonstration of a Tiered Power Management System for Economic Operation of Grid-Tied Microgrids," *IEEE Trans. Sustain. Energy,* vol. 5, pp. 1319-1327, Oct. 2014.

[5] T. Wang, D. O'Neill, and H. Kamath, "Dynamic Control and Optimization of Distributed Energy Resources in a Microgrid," *IEEE Trans. Smart Grid,* vol. 6, pp. 2884-2894, Nov. 2015.

[6] H. Kanchev, L. Di, F. Colas, V. Lazarov, and B. Francois, "Energy Management and Operational Planning of a Microgrid With a PV-Based Active Generator for Smart Grid Applications," *IEEE Trans. Ind. Electron.,* vol. 58, pp. 4583-4592, Oct. 2011.

[7] M. J. Hossain, H. R. Pota, M. A. Mahmud, and M. Aldeen, "Robust Control for Power Sharing in Microgrids With Low-Inertia Wind and PV Generators," *IEEE Trans. Sustain. Energy,* vol. 6, pp. 1067-1077, Jul. 2015.

[8] L. Nian, C. Qifang, L. Jie, L. Xinyi, L. Peng, L. Jinyong, *et al.*, "A Heuristic Operation Strategy for Commercial Building Microgrids Containing EVs and PV System," *IEEE Trans .Ind. Electron.,* vol. 62, pp. 2560-2570, Apr. 2015.

[9] K. T. Tan, X. Y. Peng, P. L. So, Y. C. Chu, and M. Z. Q. Chen, "Centralized Control for Parallel Operation of Distributed Generation Inverters in Microgrids," *IEEE Trans. Smart Grid,* vol. 3, pp. 1977-1987, Dec. 2012.

[10] W. Caisheng and H. Nehrir, "Power management of a stand-alone wind/photovoltaic/fuel-cell energy system," in *Proc. IEEE Power and Energy Society General Meeting (GM)*, 2008, pp. 1-1.

[11] A. Bidram and A. Davoudi, "Hierarchical Structure of Microgrids Control System," *IEEE Trans. Smart Grid,* vol. 3, pp. 1963-1976, May 2012.

[12] F. Katiraei, M. R. Iravani, and P. W. Lehn, "Small-signal dynamic model of a micro-grid including conventional and electronically interfaced distributed resources," *IET Gener. Transm. Distrib.,* vol. 1, pp. 369-378, May 2007.

[13] T. Dragicevic, J. M. Guerrero, J. C. Vasquez, and D. Skrlec, "Supervisory Control of an Adaptive-Droop Regulated DC Microgrid With Battery Management Capability," *IEEE Trans. Power Electron.,* vol. 29, pp. 695-706, Feb. 2014.

[14] L. Xiaonan, S. Kai, J. Guerrero, and H. Lipei, "SoC-based dynamic power sharing method with AC-bus voltage restoration for microgrid applications," in *Proc. 38th Annu. Conf. IEEE Ind. Electron. Soc. (IECON)*, 2012, pp.5682-5677 .

[15] L. Xiaonan, S. Kai, J. M. Guerrero, J. C. Vasquez, and H. Lipei, "Double-Quadrant State-of-Charge-Based Droop Control Method for Distributed Energy Storage Systems in Autonomous DC Microgrids," *IEEE Trans. Smart Grid,* vol. 6, pp. 147-157, Jan. 2015.

[16] W. Dan, T. Fen, T. Dragicevic, J. C. Vasquez, and J. M. Guerrero, "Autonomous Active Power Control for Islanded AC Microgrids With Photovoltaic Generation and Energy Storage System," *IEEE Trans. Energy Convers.,* vol. 29, pp. 882-892, Dec. 2014.

[17] A. Urtasun, E. L. Sanchis, P. Sanchis, and L. Marroyo, "Frequency-Based Energy-Management Strategy for Stand-Alone Systems With Distributed Battery Storage," *IEEE Trans. Power Electron.,* vol. 30, pp. 4794-4808, Sept. 2015.

[18] H. Mahmood, D. Michaelson, and J. Jin, "Decentralized Power Management of a PV/Battery Hybrid Unit in a Droop-Controlled Islanded Microgrid," *IEEE Trans. Power Electron.,* vol. 30, pp. 7215-7229, Dec. 2015.

[19] H. Mahmood, D. Michaelson, and J. Jin, "A Power Management Strategy for PV/Battery Hybrid Systems in Islanded Microgrids," *IEEE Trans. Emerg. Sel. Topics Power Electron.,* vol. 2, pp. 870-882, Dec. 2014.

[20] A. Bidram, A. Davoudi, and F. L. Lewis, "A Multiobjective Distributed Control Framework for Islanded AC Microgrids," *IEEE Trans. Ind. Informat.,* vol. 10, pp. 1785-1798, Aug. 2014.

[21] A. Bidram, F. L. Lewis, and A. Davoudi, "Distributed Control Systems for Small-Scale Power Networks: Using Multiagent Cooperative Control Theory," *IEEE Control Syst. Mag.,* vol. 34, pp. 56-77, Dec. 2014.

[22] Q. Shafiee, J. M. Guerrero, and J. C. Vasquez, "Distributed Secondary Control for Islanded Microgrids-A Novel Approach," *IEEE Trans. Power Electron.,* vol. 29, pp. 1018-1031, Feb. 2014.

[23] W. Dan, T. Dragicevic, J. C. Vasquez ,J. M. Guerrero, and G. Yajuan, "Secondary coordinated control of islanded microgrids based on consensus algorithms," in *Proc. Energy Conv. Cong. Expo. (ECCE)*, 2014, pp. 4290-4297.

[24] C. Ahumada, C. R, Rdenas, S. D, et al., "Secondary Control Strategies for Frequency Restoration in Islanded Microgrids With Consideration of Communication Delays," *IEEE Trans. Smart Grid*, vol. 7, pp. 1430-1441, May 2016.

[25] J. Schiffer, T. Seel, J. Raisch, and T. Sezi, "Voltage Stability and Reactive Power Sharing in Inverter-Based Microgrids With Consensus-Based Distributed Voltage Control," *IEEE Trans. Control Syst. Technol.,* vol. PP, pp. 1-1, Apr. 2015.

[26] X. Yinliang, Z. Wei, G. Hug, S. Kar, and L. Zhicheng, "Cooperative Control of Distributed Energy Storage Systems in a Microgrid," *IEEE Trans. Smart Grid,* vol. 6, pp. 238-248, Jan. 2015.

[27] Y. Wang, K. T. Tan, X. Y. Peng, and P. L. So, "Coordinated Control of Distributed Energy-Storage Systems for Voltage Regulation in Distribution Networks," *IEEE Trans. Power Del*., vol. 31, pp. 1132-1141, Jun. 2016.

[28] G. Mokhtari, G. Nourbakhsh, and A. Ghosh, "Smart Coordination of Energy Storage Units (ESUs) for Voltage and Loading Management in Distribution Networks," *IEEE Trans. Power Syst.,* vol. 28, pp. 4812-4820, Nov. 2013.

[29] Q. Shafiee, T. Dragicevic, F. Andrade, J. C. Vasquez, and J. M. Guerrero, "Distributed consensus-based control of multiple DC-microgrids clusters," in *Proc. 40th Annu. Conf. IEEE Ind. Electron. Soc. (IECON)*, 2014, pp. 2056-2062.

[30] L. Chendan, T. Dragicevic, J. C. Vasquez, J. M. Guerrero, and E. A. A. Coelho, "Multi-agent-based distributed state of charge balancing control for distributed energy storage units in AC microgrids," in *Proc. 30th IEEE Appl. Power Electron. Conf. Expo. (APEC)*, 2015, pp. 2967-2973.

[31] Q. Shafiee, T. Dragicevic, J. C. Vasquez, and J. M. Guerrero, "Hierarchical Control for Multiple DC-Microgrids Clusters," *IEEE Trans. Energy Convers.,* vol. 29, pp. 922-933, Dec. 2014.

[32] M. S. Golsorkhi and D. D. C. Lu, "A Control Method for Inverter-Based Islanded Microgrids Based on V-I Droop Characteristics," *IEEE Trans. Power Del.,* vol. 30, pp. 1196-1204, Jun. 2015.

[33] M. S. Golsorkhi and D. D. C. Lu, "A Decentralized Control Method for Islanded Microgrids Under Unbalanced Conditions," *IEEE Trans. Power Del.*, vol. 31, pp. 1112-1121, Jun. 2016.

[34] M. S. Golsorkhi and D. D. C. Lu, "A decentralized power flow control method for islanded microgrids using V-I droop," in *Proc. Iranian Conference on Electrical Engineering (ICEE)*, 2014, pp. 604-609.

[35] M. S. Golsorkhi and D. D. C. Lu, "A decentralized negative sequence compensation method for islanded mirogrids," in *Proc. International Symposium on Power Electronics for Distributed Generation Systems (PEDG)*, 2015, pp. 1-7.

[36] M. S. Golsorkhi, D. D. C. Lu, M. Savaghebi, J. C. Vasquez, and J. M. Guerrero, "A GPS-based control method for load sharing and power quality improvement in microgrids," in *Proc. International Power Electronics and Motion Control Conference (IPEMC-ECCE Asia), 2016*, pp. 3734-3740.

[37] M. Golsorkhi, D. Lu, and J. Guerrero, "A GPS-Based Decentralized Control Method for Islanded Microgrids," *IEEE Trans. Power Electron.*, Early Access, Apr. 2016.

[38] R. Olfati-Saber, J. A. Fax, and R. M. Murray, "Consensus and Cooperation in Networked Multi-Agent Systems," *in Proceedings of the IEEE* ,vol. 95, pp. 215-233, Jan. 2007.

[39] D. P. Spanos, R. Olfati-Saber, and R. M. Murray, "Dynamic consensus on mobile networks," in *IFAC world congress*, 2005, pp. 1-6.

[40] J. W. Simpson-Porco, Q. Shafiee, F. Dorfler, J. C. Vasquez, J. M. Guerrero, and F .Bullo, "Secondary Frequency and Voltage Control of Islanded Microgrids via Distributed Averaging," *IEEE Trans. Ind. Electron.,* vol. 62, pp. 7025-7038, Nov. 2015.

[41] R. Wei and R. Beard, "Distributed Consensus in Multi-vehicle Cooperative Control Theory and Applications," ed: London: Springer-Verlag, 2008.

[42] F. Xiao and L. Wang, "Asynchronous Consensus in Continuous-Time Multi-Agent Systems With Switching Topology and Time-Varying Delays," *IEEE Trans. on Autom. Control,* vol. 53, pp. 1804-1816, Sept. 2008.
[43] O. Rojo, R. Soto, and H. Rojo, "An always nontrivial upper bound for Laplacian graph eigenvalues," *Linear Algebra and its Applications,* vol. 312, pp. 155-159, Jun. 2000.
[44] L. Meng, A. Luna, D. E. R Ed, B. Sun*, et al.*, "Flexible System Integration and Advanced Hierarchical Control Architectures in the Microgrid Research Laboratory of Aalborg University," *IEEE Trans. on Ind. Appl.,* vol. 52, pp. 1736-1749, Mar. 2016.

Mohammad S. Golsorkhi (S'13) received the B.Sc. (Hons.) degree in electrical engineering from Isfahan University of Technology, Isfahan, Iran, in 2009 and the M.Sc. (Hons.) degree in electrical engineering from Tehran Poly-echnique, Tehran, Iran, in 2012. During 2011-2012, he worked in Behrad consulting engineers as a R&D engineer. His responsibilities included project management, design of power electronics devices, and power quality analysis for major industries. He is currently pursuing the PhD degree in electrical engineering at The University of Sydney, Australia. In 2015, he was a visiting PhD student with the Department of Energy Technology, Aalborg University, Denmark. His current research interests include control of microgrids, renewable energy resources, and power electronics.

Qobad Shafiee (S'13-M'15) received the MSc. degree in electrical engineering from the Iran University of Science and Technology, Tehran, Iran, in 2007, and the PhD degree in electrical engineering from the Department of Energy Technology, Aalborg University, Aalborg, Denmark, in 2014. He worked with Department of Electrical and Computer Engineering, University of Kurdistan, Sanandaj, Iran, from 2007 to 2011, where he is currently working as an assistant professor. From March 2014 to June 2014, he was a visiting scholar at the Electrical Engineering Department, University of Texas-Arlington, Arlington, TX, USA. He worked as a postdoctoral fellow with the Department of Energy Technology, Aalborg University, in 2015. His main research interests include modeling, energy management, and control of Microgrids, modeling and control of power electronics converters.

Dylan Dah-Chuan Lu (M'04–SM'09) received his B.Eng.(Hons.) degree in electronic and information engineering and Ph.D. degree, both from The Hong Kong Polytechnic University, Hong Kong, in 1999 and 2004 respectively.
In 2003, he joined Power^{e}Lab Ltd. as a Senior Design Engineer. His major responsibilities included project development and management, custom circuit design, and contribution of research in power electronics. In 2006, he joined the School of Electrical and Information Engineering, The University of Sydney, Australia, as a Lecturer and was promoted to Associate Professor in 2016. He was a Visiting Associate Professor at The University of Hong Kong in 2013. Since July 2016, he has been with the School of Electrical, Mechanical and Mechatronic Engineering, University of Technology, Sydney, Australia, where he is currently an Associate Professor. His current research interests include power electronics circuits and control for efficient and reliable power conversion and applications such as renewable energy systems, microgrids, motor drive and power quality improvement. He is a member of Engineers Australia.
He was the recipient of the Best Paper Award in the category of Emerging Power Electronic Technique at the *IEEE International Conference on Power Electronics and Drives Systems (PEDS)* 2015. He presently serves as an Associate Editor of the *IEEE Transactions on Circuits and Systems II* and the *IET Renewable Power Generation*. He served also as a Guest Editor of the *IEEE Transactions on Industrial Electronics*; special issue on Power Converters, Control and Energy Management for Distributed Generation in July 2015 issue.

Josep M. Guerrero (S'01-M'04-SM'08-FM'15) received the B.S. degree in telecommunications engineering, the M.S. degree in electronics engineering, and the Ph.D. degree in power electronics from the Technical University of Catalonia, Barcelona, in 1997, 2000 and 2003, respectively. Since 2011, he has been a Full Professor with the Department of Energy Technology, Aalborg University, Denmark, where he is responsible for the Microgrid Research Program. From 2012 he is a guest Professor at the Chinese Academy of Science and the Nanjing University of Aeronautics and Astronautics; from 2014 he is chair Professor in Shandong University; from 2015 he is a distinguished guest Professor in Hunan University; and from 2016 he is a visiting professor fellow at Aston University, UK, and a guest Professor at the Nanjing University of Posts and Telecommunications.
His research interests is oriented to different microgrid aspects, including power electronics, distributed energy-storage systems, hierarchical and cooperative control, energy management systems, smart metering and the internet of things for AC/DC microgrid clusters and islanded minigrids; recently specially focused on maritime microgrids for electrical ships, vessels, ferries and seaports. Prof. Guerrero is an Associate Editor for the IEEE TRANSACTIONS ON POWER ELECTRONICS, the IEEE TRANSACTIONS ON INDUSTRIAL ELECTRONICS, and the IEEE Industrial Electronics Magazine, and an Editor for the IEEE TRANSACTIONS on SMART GRID and IEEE TRANSACTIONS on ENERGY CONVERSION. He has been Guest Editor of the IEEE TRANSACTIONS ON POWER ELECTRONICS Special Issues: Power Electronics for Wind Energy Conversion and Power Electronics for Microgrids; the IEEE TRANSACTIONS ON INDUSTRIAL ELECTRONICS Special Sections: Uninterruptible Power Supplies systems, Renewable Energy Systems, Distributed Generation and Microgrids, and Industrial Applications and Implementation Issues of the Kalman Filter; the IEEE TRANSACTIONS on SMART GRID Special Issues: Smart DC Distribution Systems and Power Quality in Smart Grids; the IEEE TRANSACTIONS on ENERGY CONVERSION Special Issue on Energy Conversion in Next-generation Electric Ships. He was the chair of the Renewable Energy Systems Technical Committee of the IEEE Industrial Electronics Society. He received the best paper award of the IEEE Transactions on Energy Conversion for the period 2014-2015, and the best paper award of IEEE-PES in 2015. In 2014 and 2015 he was awarded by Thomson Reuters as Highly Cited Researcher, and in 2015 he was elevated as IEEE Fellow for his contributions on "distributed power systems and microgrids."